The Isoflavone Puerarin Exerts Anti-Tumor Activitiy in Pancreatic Ductal Adenocarcinoma by Suppressing Akt/mTOR Activity

Hengyue Zhu
Wenzhou Medical University First Affiliated Hospital: The First Affiliated Hospital of Wenzhou Medical University

Hong Lu
Wenzhou Medical College First Affiliated Hospital: The First Affiliated Hospital of Wenzhou Medical University

Yanyi Xiao
Wenzhou Medical University First Affiliated Hospital: The First Affiliated Hospital of Wenzhou Medical University

Hangcheng Guo
Wenzhou Medical University First Affiliated Hospital: The First Affiliated Hospital of Wenzhou Medical University

Yangyang Guo
Wenzhou Medical University First Affiliated Hospital: The First Affiliated Hospital of Wenzhou Medical University

Youze Huang
Zhejiang Chinese Medical University Affiliated Wenzhou Hospital of Traditional Chinese Medicine

Xiaodong Liu
Wenzhou Medical University

Yunfeng Shan
Wenzhou Medical University First Affiliated Hospital: The First Affiliated Hospital of Wenzhou Medical University

Yongheng Bai
Wenzhou Medical University First Affiliated Hospital: The First Affiliated Hospital of Wenzhou Medical University

Xiangyang Lin (linxy1968@126.com)
Wenzhou Medical University First Affiliated Hospital: The First Affiliated Hospital of Wenzhou Medical University

---

Research

Keywords: Puerarin, Pancreatic ductal adenocarcinoma, Glucose metabolism, Akt/mTOR

DOI: https://doi.org/10.21203/rs.3.rs-152446/v1

Abstract

Background: Puerarin (7,4'-dihydroxyisoflavone-8-β-glucopyranoside) is a natural flavonoid compound isolated from the traditional Chinese herb *Radix puerariae*. Recent studies have demonstrated that puerarin has potential anti-tumor effects via induction of apoptosis and inhibition of proliferation. However, the effect and molecular mechanism of puerarin in pancreatic ductal adenocarcinoma (PDAC) remains unknown.

Methods: The effects of puerarin on the proliferation, apoptosis, migration and invasion of pancreatic cancer cells (PCCs), and tumor growth and metastasis in PDAC xenograft mouse model were performed. In addition, Akt/mTOR signaling activity was evaluated both *in vivo* and *in vitro*.

Results: Puerarin treatment significantly repressed PCC proliferation in concentration- and time-dependent manners. Puerarin induced the mitochondrial-dependent apoptosis of PCCs by causing a Bcl-2/Bax imbalance. Moreover, puerarin inhibited PCC migration and invasion by antagonizing epithelial-mesenchymal transition (EMT). In nude mouse model, PDAC growth and metastasis were reduced by puerarin administration. Mechanistically, puerarin exerted its therapeutic effects on PDAC by suppressing Akt/mTOR signaling. Importantly, puerarin bound to the kinase domain of mTOR protein, affecting the activity of the surrounding amino acid residues associated with the binding of the ATP-Mg^{2+} complex. Further studies showed that the inhibitory effects of puerarin on PCCs were abolished by a mTOR activator MHY1485, indicating a crucial role of mTOR in anti-tumor effects of puerarin in PDAC. As a result, puerarin hindered glucose uptake and metabolism by downregulating the oxygen consumption rate (OCR) and the extracellular acidification rate (ECAR) dependent upon HIF-1α and glucose transporter GLUT1.

Conclusion: Puerarin has therapeutic potential for the treatment of PDAC by suppressing Akt/mTOR activity.

Background

Pancreatic ductal adenocarcinoma (PDAC) is the most common exocrine pancreatic cancer seen clinically. It is the fourth-leading cause of cancer-related death in the United States, second only to colorectal cancer in gastrointestinal-related deaths [1]. According to the World Health Organization (WHO) GLOBOCAN database and the 2017 Global Burden of Disease Study, PDAC is the seventh leading cause of cancer death in men and women worldwide [2]. Surgical resection is the only possible cure. Unfortunately, due to the late discovery, only 15–20% of PDAC patients are eligible for a pancreatectomy. However, even after complete resection, the prognosis of PDAC patients is poor. After resection margin-negative (R0) pancreaticoduodenectomy, the five-year survival rate of PDAC patients is about 30% for lymph node-negative and 10% for lymph node-positive patients [3, 4]. The median survival of patients with untreated and unresectable locally advanced PDAC is 8–12 months, while the median survival of patients with metastatic disease at presentation is only 3–6 months. Systemic chemotherapy can

improve the survival rate of patients with locally advanced and metastatic PDAC. In today's modern treatment era, the FOLF NO × regimen (fluorouracil + leucovorin, irinotecan, and oxaliplatin) has achieved the best outcome, but the median patient survival time is only 11.1 months [5]. New drugs, new drug targets, and new, more effective chemotherapy regimens are desperately needed in all settings.

Puerarin is a white crystal extracted from the roots of the kudzu plant or the kudzu vine. Its chemical name is 7,4'-dihydroxyisoflavone-8-β-glucopyranoside, and its molecular formula is $C_{21}H_{20}O_9$ [6]. Puerarin is the most abundant secondary metabolite, which was isolated from the rhizome of *Pueraria lobata* in the 1950s and is known as Asian ginseng. Since then, extensive research has been conducted on its pharmacological properties. Puerarin has various pharmacological effects, such as enhancing circulatory system function, reducing myocardial oxygen consumption, decreasing blood sugar, and preventing hypertension and arteriosclerosis. Anti-liver toxicity, anti-inflammatory, expectorant, antipyretic, immunity-enhancing, antibacterial, and antiviral activities have also been demonstrated [7–9]. Its low toxicity and wide range of pharmacological effects have attracted the attention of domestic and foreign researchers. In recent years, the anti-cancer effect of puerarin has been widely studied. Many studies showed that puerarin had good anti-tumor activity in animal model and many cancer cell lines [10]. However, the role of puerarin in PDAC has not been studied in-depth and needs to be further explored.

In this study, we used *in vitro* and *in vivo* experiments to investigate the anti-tumor effects of puerarin. Real-time cell analysis (RTCA), the Cell Counting Kit-8 (CCK-8) assay, colony formation, and flow cytometry analysis were used to analyze the effects of puerarin on the proliferation and apoptosis of PCCs. The transwell invasion assay, the wound healing assay, and immunocytochemical staining were used to evaluate the effects of puerarin on cell migration and invasion, and the epithelial-mesenchymal transition (EMT) of PCCs. Moreover, the effects of puerarin on the activity of Akt/mTOR and glucose metabolism were also investigated. We found that puerarin inhibited the proliferation of PCCs, induced mitochondrial-dependent apoptosis, and suppressed invasion and migration by reversing EMT. In nude mouse model, PDAC growth and metastasis were reduced by puerarin treatment. Mechanically, the activity of Akt/mTOR in PCCs and PDAC tissue was suppressed by puerarin treatment via binding to the kinase domain of mTOR protein, resulting in the inhibition of glucose metabolism by decreasing HIF-1α and GLUT1 expression. Further studies showed that the small molecule activator of mTOR, MHY1485, eliminated the puerarin-mediated inhibition of PCC proliferation and EMT induction. Thus, puerarin can be a therapeutic approach to PDAC.

Methods

Cell culture and drug treatment

Human PCC lines PANC-1 and PATU-8988T were purchased from the Cell Bank of the Chinese Academy of Sciences (Shanghai, China). The cells were cultured in Dulbecco's modified Eagle's medium (DMEM, Invitrogen, Carlsbad, CA, USA) supplemented with 10% fetal bovine serum (FBS, Invitrogen) and 1% penicillin/streptomycin (Invitrogen). The cultured cells at a density of 1×10^6 were initially plated in a 10-

cm dish for 24 h. After incubation for 24 h, the culture medium was replaced with serum-free medium. PANC-1 and PATU-8988T cells were treated with 0.2 and 0.5 mM puerarin (Fig. 1a, CAS#: 3681-99-0, Purity: ≥ 98% by HPLC, Yuanye Biotechnology, Shanghai, China) with or without MHY1485 (CAS#: 326914-06-1, MedChem Express, Monmouth Junction, NJ, USA).

Cell counting Kit-8 (CCK-8) assay

The CCK-8 assay kit (Dojindo, Shanghai, China) was used to detect the anti-tumor activity of puerarin in PANC-1 and PATU-8988T cells according to the manufacturer's instructions. First, the cells were cultured in 6-cm dishes with fresh medium for 24 h. The cells in the logarithmic growth stage were inoculated into 96-well plates at a density of 5×10^3 cells/ml. Then, the cells were treated with different concentrations of puerarin for 24 h. After that, 10 μl of CCK-8 medium and 10 μl of CCK-8 were added and the plates were incubated for another 4 h. The absorbance was measured at a wavelength of 450 nm using a microplate reader. Statistical analyses were performed using Stata statistical software (StataCorp LP). Each experiment was repeated thrice and the average value was taken as the final result.

Flow cytometry analysis

The cells were serum-starved for 24 h and the medium was replaced with complete medium. PANC-1 and PATU-8988T cells were exposed to culture medium containing different concentrations of puerarin for 24 h, and cells in the standard control group were treated with dimethyl sulfoxide (DMSO, Sigma-Aldrich, St. Louis, MO, USA). After centrifugation to collect the cells, quantification of the apoptotic cells was performed using an Annexin V-FITC Apoptosis Detection Kit (Multisciences, Hangzhou, China) according to the manufacturer's instructions. Cell apoptosis was assessed by flow cytometry (Ex = 488 nm; Em = 530 nm, BD FACSVerse™, BD Biosciences, San Jose, CA, USA), and the results were analyzed using FlowJo (TreeStar, Ashland, OR, USA).

Real-time cellular analysis (RTCA)

Cell proliferation was monitored by the xCELLigence RTCA MP System (ACEA Biosciences, San Diego, CA, USA) using 16-well E-Plates (ACEA Biosciences). The cells were seeded in triplicate at 5×10^3 cells/well in the plates. For the RTCA experiments, the cells were treated with puerarin after reaching steady growth (24 h). Impedance was measured every 15 min over 96 h and represented as the cell index by the RTCA-integrated software of the xCELLigence System. The cell index was normalized to 1 at the time point of drug administration. From this data, real-time cell growth curves were generated with GraphPad Prism 7 (GraphPad Software, La Jolla, CA, USA).

Transwell invasion assay

Transwell assays were performed using Transwell chambers (Costar, New York City, NY, USA) with Matrigel® (BD Biosciences). After treatment with various concentrations of puerarin for 24 h, cell suspensions were prepared using ethylenetetraacetic acid (EDTA) enzyme. The cells were resuspended in serum-free medium and transferred to the inner chamber (5×10^4 cells per chamber). Complete medium

was added to the outer chamber, and the plate was incubated in a CO_2 incubator (37 ℃) for observation for 12 h. After carefully removing the non-migrating cells at the membrane site with a cotton swab, the cells were fixed with formaldehyde and stained with 0.1% crystal violet (Sigma), and quantification was performed by counting five random fields under the microscope (Leica Microsystems, Wetzlar, Germany). Each experiment was repeated three times.

Colony formation assay

The cells were seeded into 6-well plates at 1×10^3 cells per well and treated with puerarin 24 h later. After 24 h, the media was replaced with fresh media and cultured for 14 days. The colonies were then fixed with 2% formaldehyde and stained with 0.5% crystal violet. The number of colonies with ≥ 50 cells was counted under a microscope.

Wound healing assay

PANC-1 or PATU-8988T cells were seeded in 6 well plates and maintained at 37 ℃ for 24 h. The cells were scratched using a crystal pipette tip to make a linear gap. Next, the detached cells were washed away with phosphate-buffered saline (PBS) and different concentrations of puerarin were added. The cells were allowed to fill the gap, and after 24 h, images of the areas were captured using a microscope (Leica Microsystems).

Immunocytochemical staining

Immunofluorescence staining was performed based on established protocols. PANC-1 and PATU-8988T cells with different treatments were grown on glass coverslips for 24 h. The cells were fixed with 4% formaldehyde and permeabilized with 0.1% Triton X-100 (Thermo Scientific, Waltham, MA, USA). Blocking was performed with 4% goat serum (Gibco, Thermo Fisher Scientific) in Dulbecco's phosphate-buffered saline (DPBS; Invitrogen, Paisley, UK) for 1.5 h at 37 ℃, followed by incubation with the primary antibodies (Table S1): anti-Ki67 (1:200), anti-α-SMA (1:200), anti-E-cadherin (1:200), and anti-p-mTOR (1:200) at 4℃ overnight. Next, the membranes were incubated in the appropriate second antibodies for 1 h at room temperature. At least three independent experiments for immunofluorescence staining were conducted.

Western blot analysis

After treating the cells for 24 h, the cells in each group were collected and the total cellular protein was extracted. After separation by sodium dodecyl sulfate-polyacrylamide gel electrophoresis (SDS-PAGE), the proteins were transferred onto polyvinylidene fluoride (PVDF) membranes. The membranes were blocked with 5% non-fat milk for 1 h at room temperature and incubated overnight at 4 ℃ with the primary antibodies (Table S1). The membranes were washed three times in Tris-buffered saline with 0.1% Tween 20 (TBST) the following day and incubated with the second antibody (anti-rabbit IgG) at room temperature for 1 h. After the membranes were rinsed, the protein expression levels were detected by enhanced chemiluminescence (ECL) and visualized by autoradiography. GAPDH was used as the internal reference protein.

Glucose metabolism assay

The intact cellular oxygen consumption rate (OCR) and extracellular acidification rate (ECAR) were measured using a Seahorse XF96 Extracellular Flux Analyzer (Seahorse Bioscience, North Billerica, MA, USA). Briefly, 1 ×10^4 PANC-1 and PATU-8988T cells were seeded into 96-well cell plates and incubated overnight at 37 ℃ at 5% CO_2. Both cells were pretreated with or without different concentrations of puerarin for 24 h. Simultaneously, the calibration plates were incubated overnight at 37 ℃ in a non-CO_2 incubator, then the cell medium was replaced with assay medium. Once the probe calibration was completed, the cell plate replaced the probe plate. The analyzer plotted the OCR value, followed by the injection of the compounds sequentially as follows: oligomycin (an inhibitor of ATP synthase; 2.5 μM), carbonyl cyanide 4-(trifluoromethoxy) phenylhydrazone (FCCP, an uncoupler of OXPHOS; 2 μM), rotenone (an inhibitor of complex I; 0.25 μM), and anti-mildew A (an inhibitor of complex III; 0.25 μM) (n = 8). The ECAR was evaluated after the continuous injection of glucose (10 mM), oligomycin (1 μM), and 2-Deoxy-D-glucose (2-DG, 50 mM) (n = 8). After completing the test, the BCA Protein Assay Kit was used to determine the protein concentrations to normalize the OCR and the ECAR according to the manufacturer's instructions.

Nude mouse tumorigenicity

Male BALB/c nude mice (6–8 weeks old) were obtained from the Wenzhou Medical University Experimental Animal Center (Wenzhou, China). All mice were housed under controlled conditions (temperature, 21–23 ℃; 12 h light/dark cycle; 55% humidity). PANC-1 cells (3 × 10^6) in 0.2 ml PBS were subcutaneously injected into the right thighs of 10 nude mice, which were randomly divided into two groups (n = 5 in each group). Mice in the experimental group received puerarin by intragastric gavage every three days for one month. The control group received DMSO injections for one month. Tumor formation in the nude mice was monitored for 30 days, with the length and width measured every three days. The tumor size was calculated according to the standard formula: tumor volumes (cm^3) = (the longest diameter) × (the shortest diameter)^2 × 0.5. The mice were deeply anesthetized with sodium pentobarbital and euthanized by cervical dislocation.

This animal study was approved by the Institutional Animal Care and Use Committee of Wenzhou Medical University, China. The animal experiments were conducted according to all regulatory and institutional guidelines for animal welfare (National Institutes of Health Publications, NIH Publications No. 80 − 23) [11].

Histopathological analysis

Tumor specimens from the animals were paraffin-embedded and cut into 4-μm-thick sections. Standard hematoxylin and eosin staining (HE, Yuanye Biotechnology) was performed on 4-μm sections from the paraffin-embedded tumor samples. Immunohistochemical (IHC) analysis was conducted under a microscope according to a previous method [11]. In brief, 4-μm-thick sections were dewaxed with xylene and rehydrated in a graded ethanol series. The sections were incubated in 0.1% sodium citrate buffer (pH

6.0) for antigen retrieval, and endogenous peroxidase activity was blocked with 3% hydrogen peroxide (Beyotime, China). IHC staining was performed using the following primary antibodies: anti-Ki67 (1:200), anti-c-Myc (1:200), anti-α-SMA (1:200), anti-E-cadherin (1:200), anti-cleaved caspase-8 (1:100), anti-cytochrome C (1:100), and anti-HIF-1α (1:200). The integrated optical density (IOD) was measured using Image-Pro Plus software (version 6.0, Media Cybernetics, Silver Spring, MD, USA). All samples were semi-quantitatively or quantitatively assessed by two independent investigators in a blinded manner.

Molecular docking

Molecular docking was performed as previously described [12], Puerarin and mTOR were rigidly docked, and the docking results were analyzed by PyMOL software. The puerarin molecule was downloaded from Pubchem, and the molecular energy was optimized through Chem 3D Ultra Software (8.0.3 version, Cambridge-Soft, MA, USA). The crystal structure of mTOR was downloaded from the Protein Structure Database (Protein Data Bank, PDB) (http://www.rcsb.org/pdb/), and the protein was processed by Autodock (MGLTools-1.5.6) to remove water molecules and hydrogenate and to add volume.

Database analysis

The correlation between AKT and mTOR expression and the activity of KRAS, TP53, CDKN2A, and SMAD4 was evaluated in the GEPIA 2 database website (http://gepia2.cancer-pku.cn/#analysis).

Statistical analysis

The data are expressed as the mean ± standard deviation for the *in vitro* and *in vivo* experiments. All statistical analyses were performed using GraphPad Prism statistical analysis software (version 8.0, GraphPad Software, Inc., LaJolla, CA, USA). Statistical comparisons were made with a two-sided t-test. One-way analysis of variance (ANOVA) with Bonferroni's post-hoc test was used when more than two groups were present. Statistical significance was indicated by a *P*-value of < 0.05.

Results

Puerarin inhibits PCC proliferation and induces mitochondria-mediated apoptosis

To investigate the effect of puerarin on PCC proliferation, the RTCA, CCK-8, and colony formation assays were performed. As shown in Fig. 1b and c, as expected, puerarin treatment (0.2 and 0.5 mM) significantly inhibited the growth of PANC-1 and PATU-8988T cells in concentration- and time-dependent manners. The CCK-8 assay results of the PANC-1 and PATU-8988T cells confirmed the concentration-dependent inhibition of cell growth by puerarin (Fig. 1b, c). Puerarin also significantly reduced colony formation in the PANC-1 and PATU-8988T cells (Fig. 1d). To investigate the effect of puerarin on cell proliferation, we used immunofluorescence staining for the Ki67 marker expressed by proliferating cells. The level of Ki67 protein varied with the cell cycle and was higher in the G2/M phase and lower in the

G0/G1 phase [13]. In the PANC-1 and PATU-8988T cell lines, we observed a decrease in Ki67 protein expression in both the PANC-1 and PATU-8988T cells treated with puerarin (Fig. 1e) compared to the control cells. Therefore, the above results suggest that puerarin inhibited PCC proliferation in concentration- and time-dependent manners.

Next, we evaluated the effects of puerarin on PCC apoptosis by flow cytometry analysis. Puerarin treatment significantly increased the proportion of apoptotic and necrotic cells (Fig. 1g). Further studies showed an increase in caspase-8 in both the PANC-1 and PATU-8988T cells treated with puerarin (Fig. 1h). Apoptosis in cancer cells depends upon the dynamic equilibrium of Bax and Bcl-2 expression [14]. Puerarin was observed to increase Bax expression and decrease Bcl-2 expression (Fig. 1h). These results suggest that puerarin induced the death receptor- and mitochondrial-mediated apoptosis of PCCs.

Puerarin inhibits the migration and invasion of PCCs by antagonizing epithelial-mesenchymal transition

Enhanced cell migration and invasion abilities underlie PCC metastasis mechanisms, resulting in poor prognosis [15]. Here, puerarin reduced the migration rate of PANC-1 and PATU-8988T cells as determined by the scratch wound assay (Fig. 2a, b) and the effect was concentration-dependent as well as time-dependent. Also, puerarin treatment significantly inhibited the numbers of invading PANC-1 and PATU-8988T cells detected by the transwell assay (Fig. 2c, d). Further studies showed that puerarin decreased the protein level of α-SMA in PANC-1 and PATU-8988T cells and increased the E-cadherin protein level (Fig. 2e). Immunofluorescence analysis revealed the downregulated expression of α-SMA and the increased expression of E-cadherin after puerarin treatment (Fig. 2f). In general, these results suggest that puerarin inhibited PCC migration and invasion by inhibiting EMT and tumor mammosphere formation.

Puerarin suppresses PDAC growth and metastasis in vivo

To determine the anticancer effects of puerarin *in vivo*, nude mice were injected with PANC-1 cells and then administrated puerarin or saline as a control. Figure 3a shows the morphology of tumor xenografts changes in the experimental group after puerarin treatment. We found that the administration of puerarin significantly reduced tumor volume and weight (Fig. 3c, d). The pathological results in the PDAC model tissue were shown by HE staining. Further studies showed that puerarin administration upregulated the expression of cleaved caspase-8 (Fig. 3g, h). Also, puerarin increased Bax expression and decreased Bcl-2 expression (Fig. 3g). A decrease in the expression of Ki67 was observed in the tumor tissue (Fig. 3e). Therefore, our *in vivo* findings suggest that puerarin induced PCC apoptosis through death receptor- and mitochondrial-mediated pathways. To assess whether puerarin inhibited PDAC migration, we examined the expression of EMT process-related proteins. The results showed that puerarin decreased α-SMA expression and increased E-cadherin expression (Fig. 3i). It also reduced the expression of c-Myc, an oncoprotein associated with tumor progression and drug resistance (Fig. 3f) [16]. Hypoxia is usually observed in PDAC and some other solid tumors. HIF-1α protein, a key regulator of the hypoxia response, was found to accumulate in PDAC tissues. Several studies have shown that hypoxia was an independent predictor of poor prognosis [17]. We observed the downregulation of HIF-1α protein after puerarin

treatment (Fig. 3j). In summary, these data suggest that puerarin inhibited the growth and metastasis of PDAC in a mouse xenograft model.

Puerarin reduces the activity of Akt/mTOR signaling in vitro **and** in vivo

Anticancer effects involve many mechanisms, including oxidative stress, intrinsic and extrinsic mechanisms, as well as the survivin, PI3K/Akt/mTOR, SHH [18], Nrf2/Keap1 [19], inflammation, and autophagy pathways [20]. Studies have shown that the signal transduction pathway mediated by phosphatidylinositol 3 kinase (PI3K) was closely related to cancer occurrence. Many downstream molecules make up the PI3K/Akt signal pathway, including mTOR, one of the more important targets of rapamycin. mTOR signaling plays a crucial role in cell growth, protein translation, autophagy, and metabolism [21]. The activation of mTOR contributes to the pathogenesis of various tumors. We also found that these PCCs exhibited heterogeneous PI3K/Akt/mTOR pathway activation at the protein level (Fig. 4c). In this study, we investigated the effect of puerarin on mTOR activity in PANC-1 and PATU-8988T cells. We found that puerarin suppressed the mTOR signaling pathway (Fig. 4d, e), suggesting that mTOR may be a target of puerarin. Puerarin-induced the downregulation of phosphorylated mTOR expression in PANC-1 and PATU-8988T cells (Fig. 4f, g). The *in vitro* experiments confirmed that puerarin inhibited the overexpression of mTOR in PDAC tissues (Fig. 4h, i).

Puerarin binds to the kinase domain of mTOR protein to inhibit protein activity

To further analyze the biochemical pathways of puerarin affecting mTOR protein, we used Autodock (MGLTools-1.5.6) to rigidly dock puerarin with the FAT domain (blue cartoon) and the kinase domain (KD, green cartoon) areas of mTOR (Fig. 5a). We found that the possible binding sites of puerarin and mTOR included two structural regions i and ii (Fig. 5b, c), with binding energies of -5.17 and − 7.0, respectively. Figure 5d shows that there were many ATP-Mg complex binding-related amino acid residues around the i and ii binding sites. Once puerarin binds to the i and ii sites on mTOR protein, it may affect the activity of the above amino acid residues, and then affect mTOR activation activity.

Activated mTOR signaling eliminates puerarin-mediated anti-tumor effects

Given the anti-tumor effect of puerarin on PDAC by inhibiting mTOR signal transduction, we next investigated whether activated mTOR signal transduction influenced this effect of puerarin. In the PANC-1 and PATU-8988T cells, we used MHY1485, a significant cell permeability mTOR activator to activate the mTOR pathway, targeting the ATP domain mTOR. The activation of mTOR signaling eliminated the anti-proliferative effect of puerarin as determined by the colony formation test (Fig. 6a, b). Using the transwell and wound healing assays, we demonstrated that MHY1485 treatment increased the invasion and migration rates of the PANC-1 and PATU-8988T cells (Fig. 6d-g). Thus, activated mTOR signaling eliminated puerarin-mediated EMT suppression, as shown by the increased expression of α-SMA,

vimentin, Snail1, and Slug (Fig. 6h, i). These findings confirmed that mTOR signaling played a crucial role in the anti-tumor effect of puerarin in PDAC.

Puerarin inhibits mTOR-mediated glucose metabolism in PCCs

To satisfy the need for rapid proliferation, tumor cells need more energy, so the process of bioenergy metabolism targeting tumor cells is a new therapeutic strategy to inhibit the growth of tumor cells [22]. A bioenergy analyzer was used to measure the corresponding OCR and ECAR, and the effects of external factors on mitochondrial uptake and glycolysis were analyzed statistically. The primary respiration, ATP production, maximum respiration, and spare respiration of cells treated with puerarin decreased significantly (Fig. 7a-d), indicating that puerarin inhibited the energy metabolism of the mitochondria. The glycolysis of the tumor cells treated with puerarin was significantly inhibited (Fig. 7e, g). The results showed that the basal glycolysis rate and the compensatory glycolysis rate decreased significantly (Fig. 7f, h). Further studies showed that GLUT1 and HIF-1α protein expression was inhibited (Fig. 7i). Considering the close connection between puerarin and the mTOR pathway, our research results indicate that puerarin may regulate downstream GLUT1 through the mTOR pathway and affect tumor cell metabolism.

Discussion

Puerarin has certain anti-cancer effects in a variety of tumors. However, its role in PDAC is still poorly understood. In the present study, we showed that puerarin treatment significantly repressed the proliferation of PCCs in concentration- and time-dependent manners. In addition, puerarin induced the mitochondrial-dependent apoptosis of PCCs by causing a Bcl-2/Bax imbalance. Moreover, puerarin inhibited the migration and invasion of PCCs by antagonizing EMT. In the nude mouse model, PDAC growth and metastasis were also reduced by puerarin administration. Thus, these *in vitro* and *in vivo* results indicate that puerarin exerted effective protection against PDAC.

Previous studies have shown that puerarin impeded cell growth, blocked the cell development in the G0/G1 cell cycle phase, induced apoptosis in bladder cancer cells through the mTOR/p70 S6K signaling pathway, and suppressed cell growth and migration in HPV-positive cervical cancer cells by inhibiting the PI3K/mTOR signaling pathway [23, 24]. In addition, puerarin 6’-O-xyloside, an analog of puerarin, suppressed hepatocellular carcinoma by regulating proliferation, stemness, and apoptosis by inhibiting PI3K/Akt/mTOR [25]. However, the anti-tumor effect and molecular mechanism of puerarin in PDAC remains unknown. Here, we identified effective protection against PDAC by puerarin and showed that the Akt/mTOR signaling pathway played an important role in the anti-tumor effect of puerarin.

mTOR protein kinase is involved in many major signaling pathways and plays a key role in organizing the cellular and body physiology of all eukaryotes. In the two and a half years since its discovery, mTOR has been shown to be the central node in the network that controls cell growth. In this way, it integrates

information about the availability of energy and nutrients to coordinate the synthesis or decomposition of new cellular components. The dysregulation of this basic signal transduction pathway can disrupt cellular homeostasis and may aggravate the overgrowth of cancer and pathology related to aging and metabolic diseases [26]. Although mTOR kinase itself is rarely mutated in cancer, it is easily hijacked by upstream oncogenic nodes, including those in the PI3K/Akt pathway and the MAPK pathway driven by Ras. As a result, mTOR signaling is active in as many as 80% of human cancers. In this case, mTOR signaling plays a key role in maintaining the growth and survival of cancer cells [27]. Cancer patients with acquired drug resistance have a poor prognosis, which prompted us to explore the vulnerability of cancer cells that are resistant to chemotherapy. The mTOR pathway is located downstream of the phosphoinositide 3-kinase (PI3K) and Akt pathway regulated by the phosphatase and tensin homolog (*PTEN*) tumor suppressor gene [28]. Inhibition of the mTOR pathway can inhibit tumor progression at multiple levels. In terms of mechanism, puerarin exerts a therapeutic effect on PDAC by inhibiting Akt/mTOR signal transduction activity, as shown by a decrease in phosphorylation and nuclear transcription. Further studies showed that the small molecule activator of mTOR, MHY1485, eliminated the puerarin-mediated inhibition of PCC proliferation and apoptosis induction. Viewing mTOR as a widespread driver of therapeutic resistance suggests considerable hope for targeting cancer drug resistance using mTOR inhibitors [29]. Significantly, puerarin inhibited the phosphorylation of mTOR, the downstream expression of GLUT1 and HIF-1α, and the glucose metabolism of PCC. In PDAC, even under normoxia, glycolysis is the primary energy source for cancer cell proliferation, invasion, migration, and metastasis [30]. We found that puerarin hindered glucose uptake and metabolism by downregulating the OCR and ECAR levels that depend upon HIF-1α and the glucose transporter GLUT1. Therefore, these findings indicate that puerarin has the therapeutic potential to treat PDAC by inhibiting the energy metabolism of tumor cells. Puerarin inhibited glucose uptake and metabolism by reducing the OCR and the ECAR dependent upon HIF-1α and glucose transporter GLUT1. Further studies showed that the mTOR small molecule activator MHY1485 could eliminate the puerarin-mediated inhibition of PCC proliferation and induction of apoptosis. Therefore, these findings suggest that puerarin has therapeutic potential for PDAC by inhibiting Akt/mTOR activity. The limitation of our study was that we did not explore the specific target of puerarin in the mTOR signal pathway, which needs further study.

In response to the increasing interest in drug development, researchers have actively tried to develop new treatment strategies, including neoadjuvant chemotherapy for patients with resectable or marginally resectable incremental cancers, multi-drug combination chemotherapy for patients with advanced PDAC, and new complex drugs or immuno-oncology drugs for PDAC patients with specific gene mutations.

Bax and Bak are two pro-apoptotic proteins with similar functions in the Bcl-2 family. Because of their essential role as effectors of mitochondrial outer membrane permeability (MOMP), Bcl and Bak are the portals of apoptosis in mitochondria, an essential step in the process of dependent apoptosis [31]. We observed an imbalance in the Bcl-2/Bax ratio after puerarin treatment, which indicated that puerarin could induce the mitochondria-dependent apoptosis of PCCs.

EMT is a cellular process in which epithelial cells acquire a mesenchymal phenotype and behavior after epithelial downregulation. The cells then exhibit fibroblast-like morphology and cellular structure and increase their ability to migrate. Also, these now-migrating cells are usually invasive [32]. Metastasis-related events are the leading cause of cancer-related death, and circulating tumor cells (CTCs) play a crucial role in metastatic recurrence. The EMT marker expressed in CTCs is closely related to poor clinical results. As mentioned in previous studies, puerarin inhibits migration and invasion by antagonizing EMT [33]. We studied the effects of puerarin on PCC proliferation, apoptosis, migration, and invasion, tumor growth, and metastasis in a PDAC xenograft mouse model. In the nude mouse model, the use of puerarin reduced the growth and metastasis of PDAC.

The limitation was that this study did not thoroughly explore the specific targets of puerarin acting in the mTOR signaling pathway. At the same time, our study used two cell lines, PANC-1 and PATU-8988T, so they could not fully cover the entire range of the tumor. More importantly, a genetic approach to exploring the association between mTOR signaling and the ant-tumor effects of puerarin needs to be implemented.

Conclusion

In conclusion, our results revealed that puerarin had a clear function in pancreatic cancer. It inhibited tumor cell proliferation and migration. Interestingly, our results suggest that the mTOR signaling pathway may play an important role in the anti-tumor process of puerarin. The process also involves downregulation of the OCR and the ECAR dependent upon HIF-1α and the glucose transporter GLUT1 to inhibit glucose uptake and metabolism. In addition, puerarin inhibited the migration and invasion of PCCs by antagonizing the EMT. In the nude mouse model, puerarin inhibited the growth and metastasis of PDAC. Further studies showed that MHY1485, a small molecule activator of mTOR, could block the puerarin-mediated effect of inhibiting PCCs proliferation and inducing PCCs apoptosis (Fig. 8). Therefore, puerarin has the potential to treat PDAC by inhibiting Akt/mTOR activity.

Abbreviations

Bax, Bcl-2-associated X protein

Bcl-2, B-cell lymphoma 2

CCK-8, cell counting kit 8

DMEM, Dulbecco modified Eagle medium

ECAR, extracellular acidification rate

EMT, epithelial-mesenchymal transition

FBS, fetal bovine serum

GAPDH, glyceraldehyde 3-phosphate dehydrogenase

GLUT1, glucose transporter type 1

HIF-1α, hypoxia-inducible factor-1α

OCR, oxygen consumption rate

PCC, pancreatic cancer cell

PDAC, pancreatic ductal adenocarcinoma

RTCA, real-time cell analysis

Declarations

Acknowledgements

Not applicable

Authors' contributions

LX and BY designed the experiments; ZH and LH carried out most of the experiments; ZH, LH, XY, GY, HY, and GH analyzed the data and organized the Figures; ZH wrote the manuscript and LH reviewed it. LX and SY provided important support for the design and implementation of supplementary experiments. All authors read and approved the final manuscript.

Funding

This study was sponsored by Wenzhou Science and Technology Plan Project, China (Grant No. Y20180100) and Key Laboratory of Diagnosis and Treatment of Severe Hepato-Pancreatic Diseases of Zhejiang Province (2018E10008).

Availability of data and materials

All data generated or analyzed during this study are available from the corresponding author on reasonable request.

Ethics approval and consent to participate

Animal experiments were approved by the Committee for Animal Experiments at Wenzhou Medical University.

Consent for publication

All authors agreed on the manuscript

Competing interests

The authors declare that they have no competing interests.

Author details

[1]Key Laboratory of Diagnosis and Treatment of Severe Hepato-Pancreatic Diseases of Zhejiang Province, The First Affiliated Hospital of Wenzhou Medical University, Wenzhou 325000, China

[2]Department of Laboratory Medicine, The First Affiliated Hospital of Wenzhou Medical University, Wenzhou 325000, China

[3]Department of Laboratory Medicine, Wenzhou Hospital of Traditional Chinese Medicine, Wenzhou 325000, China

[4]Center for Health Assessment, Wenzhou Medical University, Wenzhou, 325000, China

[5]Department of Hepato-Pancreato-Biliary Surgery, The First Affiliated Hospital of Wenzhou Medical University, Wenzhou 325000, China

References

1. Siegel RL, Miller KD, Jemal A. Cancer statistics. 2019. CA Cancer J Clin. 2019; 69(1):7–34. doi: 10.3322/caac.21551.
2. Collaborators GBDPC. The global, regional, and national burden of pancreatic cancer and its attributable risk factors in 195 countries and territories, 1990–2017: a systematic analysis for the Global Burden of Disease Study 2017. Lancet Gastroenterol Hepatol. 2019;4(12):934–47. doi:10.1016/S2468-1253(19)30347-4.
3. Kang MJ, Jang JY, Chang YR, Kwon W, Jung W, Kim SW. Revisiting the concept of lymph node metastases of pancreatic head cancer: number of metastatic lymph nodes and lymph node ratio according to N stage. Ann Surg Oncol. 2014;21(5):1545–51. doi:10.1245/s10434-013-3473-9.
4. Allen PJ, Kuk D, Castillo CF, Basturk O, Wolfgang CL, Cameron JL, Lillemoe KD, Ferrone CR, Morales-Oyarvide V, He J, et al. Multi-institutional Validation Study of the American Joint Commission on Cancer (8th Edition) Changes for T and N Staging in Patients With Pancreatic Adenocarcinoma. Ann Surg. 2017; 265(1):185–191. doi: 10.1097/SLA.0000000000001763.
5. Conroy T, Desseigne F, Ychou M, Bouche O, Guimbaud R, Becouarn Y, Adenis A, Raoul JL, Gourgou-Bourgade S, de la Fouchardiere C, et al. FOLFIRINOX versus gemcitabine for metastatic pancreatic cancer. N Engl J Med. 2011;364(19):1817–25. doi:10.1056/NEJMoa1011923.
6. Luo CF, Yuan M, Chen MS, Liu SM, Ji H. Metabolites of puerarin identified by liquid chromatography tandem mass spectrometry: similar metabolic profiles in liver and intestine of rats. J Chromatogr B Analyt Technol Biomed Life Sci. 2010;878(3–4):363–70. doi:10.1016/j.jchromb.2009.12.002.

7. Li W, Xu X, Dong D, Lei T, Ou H. Up-regulation of thioredoxin system by puerarin inhibits lipid uptake in macrophages. Free Radic Biol Med. 2020. doi:10.1016/j.freeradbiomed.2020.11.011.
8. Xie W, Du L. Diabetes is an inflammatory disease: evidence from traditional Chinese medicines. Diabetes Obes Metab. 2011;13(4):289–301. doi:10.1111/j.1463-1326.2010.01336.x.
9. Pan B, Fang S, Zhang J, Pan Y, Liu H, Wang Y, Li M, Liu L. Chinese herbal compounds against SARS-CoV-2: Puerarin and quercetin impair the binding of viral S-protein to ACE2 receptor. Comput Struct Biotechnol J. 2020;18:3518–27. doi:10.1016/j.csbj.2020.11.010.
10. Ahmad B, Khan S, Liu Y, Xue M, Nabi G, Kumar S, Alshwmi M, Qarluq AW. Molecular Mechanisms of Anticancer Activities of Puerarin. Cancer Manag Res. 2020;12:79–90. doi:10.2147/CMAR.S233567.
11. Zhang X, Lu H, Xie S, Wu C, Guo Y, Xiao Y, Zheng S, Zhu H, Zhang Y, Bai Y. Resveratrol suppresses the myofibroblastic phenotype and fibrosis formation in kidneys via proliferation-related signalling pathways. Br J Pharmacol. 2019;176(24):4745–59. doi:10.1111/bph.14842.
12. Morris GM, Huey R, Lindstrom W, Sanner MF, Belew RK, Goodsell DS, Olson AJ. AutoDock4 and AutoDockTools4: Automated Docking with Selective Receptor Flexibility. J Comput Chem. 2009;30(16):2785–91. doi:10.1002/jcc.21256.
13. Gerdes J, Lemke H, Baisch H, Wacker H, Schwab U, Stein H. Cell cycle analysis of a cell proliferation-associated human nuclear antigen defined by the monoclonal antibody Ki-67. Journal of immunology (Baltimore, Md: 1950). 1984; 133(4):1710–1715. doi.
14. de Bruin E, Medema J. Apoptosis and non-apoptotic deaths in cancer development and treatment response. Cancer treatment reviews. 2008;34(8):737–49. doi:10.1016/j.ctrv.2008.07.001.
15. Beel S, Kolloch L, Apken LH, Jurgens L, Bolle A, Sudhof N, Ghosh S, Wardelmann E, Meisterernst M, Steinestel K, et al. kappaB-Ras and Ral GTPases regulate acinar to ductal metaplasia during pancreatic adenocarcinoma development and pancreatitis. Nat Commun. 2020;11(1):3409. doi:10.1038/s41467-020-17226-0.
16. Guo Y, Tong Y, Zhu H, Xiao Y, Guo H, Shang L, Zheng W, Ma S, Liu X, Bai Y. Quercetin suppresses pancreatic ductal adenocarcinoma progression via inhibition of SHH and TGF-beta/Smad signaling pathways. Cell Biol Toxicol. 2020. doi:10.1007/s10565-020-09562-0.
17. Man J, Yu X, Huang H, Zhou W, Xiang C, Huang H, Miele L, Liu Z, Bebek G, Bao S, et al. Hypoxic Induction of Vasorin Regulates Notch1 Turnover to Maintain Glioma Stem-like Cells. Cell stem cell. 2018;22(1):104–18.e106. doi:10.1016/j.stem.2017.10.005.
18. Bai Y, Bai Y, Dong J, Li Q, Jin Y, Chen B, Zhou M. Hedgehog Signaling in Pancreatic Fibrosis and Cancer. Medicine. 2016;95(10):e2996. doi:10.1097/MD.0000000000002996.
19. Wu S, Lu H, Bai Y. Nrf2 in cancers: A double-edged sword. Cancer Med. 2019;8(5):2252–67. doi:10.1002/cam4.2101.
20. Sarwar A, Wang B, Su Q, Zhang Y. MiRNAs directly targeting the key intermediates of biological pathways in pancreatic cancer. Biochem Pharmacol. 2020:114357. doi: 10.1016/j.bcp.2020.114357.
21. Moonesi M, Zaka Khosravi S, Molaei Ramshe S, Allahbakhshian Farsani M, Solali S, Mohammadi MH, Farshdousti Hagh M, Mehdizadeh H. IGF family effects on development, stability, and treatment

of hematological malignancies. J Cell Physiol. 2020. doi:10.1002/jcp.30156.

22. Xiao Z, Han L, Lee H, Zhuang L, Zhang Y, Baddour J, Nagrath D, Wood C, Gu J, Wu X, et al. Energy stress-induced lncRNA FILNC1 represses c-Myc-mediated energy metabolism and inhibits renal tumor development. Nature communications. 2017;8(1):783. doi:10.1038/s41467-017-00902-z.
23. Jia L, Hu Y, Yang G, Li P. Puerarin suppresses cell growth and migration in HPV-positive cervical cancer cells by inhibiting the PI3K/mTOR signaling pathway. Exp Ther Med. 2019;18(1):543–9. doi:10.3892/etm.2019.7589.
24. Jiang K, Chen H, Tang K, Guan W, Zhou H, Guo X, Chen Z, Ye Z, Xu H. Puerarin inhibits bladder cancer cell proliferation through the mTOR/p70S6K signaling pathway. Oncol Lett. 2018;15(1):167–74. doi:10.3892/ol.2017.7298.
25. Li L, Liu JD, Gao GD, Zhang K, Song YW, Li HB. Puerarin 6"-O-xyloside suppressed HCC via regulating proliferation, stemness, and apoptosis with inhibited PI3K/AKT/mTOR. Cancer Med. 2020;9(17):6399–410. doi:10.1002/cam4.3285.
26. Liu G, Sabatini D. mTOR at the nexus of nutrition, growth, ageing and disease. Nature reviews Molecular cell biology. 2020;21(4):183–203. doi:10.1038/s41580-019-0199-y.
27. Menon S, Manning B. Common corruption of the mTOR signaling network in human tumors. Oncogene. 2008:S43–51. doi: 10.1038/onc.2009.352.
28. Wey S, Luo B, Tseng C, Ni M, Zhou H, Fu Y, Bhojwani D, Carroll W, Lee A. Inducible knockout of GRP78/BiP in the hematopoietic system suppresses Pten-null leukemogenesis and AKT oncogenic signaling. Blood. 2012;119(3):817–25. doi:10.1182/blood-2011-06-357384.
29. Ilagan E, Manning BD. Emerging role of mTOR in the response to cancer therapeutics. Trends Cancer. 2016;2(5):241–51. doi:10.1016/j.trecan.2016.03.008.
30. Riester M, Xu Q, Moreira A, Zheng J, Michor F, Downey R. The Warburg effect: persistence of stem-cell metabolism in cancers as a failure of differentiation. Annals of oncology: official journal of the European Society for Medical Oncology. 2018;29(1):264–70. doi:10.1093/annonc/mdx645.
31. Ku B, Liang C, Jung JU, Oh BH. Evidence that inhibition of BAX activation by BCL-2 involves its tight and preferential interaction with the BH3 domain of BAX. Cell Res. 2011;21(4):627–41. doi:10.1038/cr.2010.149.
32. Yang J, Antin P, Berx G, Blanpain C, Brabletz T, Bronner M, Campbell K, Cano A, Casanova J, Christofori G, et al. Guidelines and definitions for research on epithelial-mesenchymal transition. Nat Rev Mol Cell Biol. 2020;21(6):341–52. doi:10.1038/s41580-020-0237-9.
33. Franses JW, Philipp J, Missios P, Bhan I, Liu A, Yashaswini C, Tai E, Zhu H, Ligorio M, Nicholson B, et al. Pancreatic circulating tumor cell profiling identifies LIN28B as a metastasis driver and drug target. Nat Commun. 2020;11(1):3303. doi:10.1038/s41467-020-17150-3.

Figures

Figure 3

Puerarin inhibits the tumor growth and metastasis of PDAC in animal xenograft model. A Effects of puerarin on morphologic changes in the experimental groups. B Pathological results of HE staining for PDAC in tissues of the model group. Bar = 50 μm. C Effect of puerarin on the volume of tumors in the animal xenograft model. D Effects of puerarin on tumor weight. E Immunohistochemical (IHC) staining for Ki67 in the puerarin-treated model. Bar = 50 μm. F IHC staining for c-Myc in the puerarin-treated model. Bar = 50 μm. G Western blot analysis showing the expression of cleaved caspase-8, Bax and Bcl-2 in PANC-1 and PATU-8988T cells with or without puerarin treatment. H IHC staining for cleaved caspase-8 and cytochrome C in the puerarin-treated model. Bar = 50 μm. I IHC staining for E-cadherin and α-SMA in the puerarin-treated model. Bar = 50 μm. J IHC staining for HIF-1α in the puerarin-treated model. Bar = 50 μm. The data are presented as the mean ± standard deviation, and were analyzed by a two-sided Student's t-test. *P < 0.05 and ***P < 0.001.

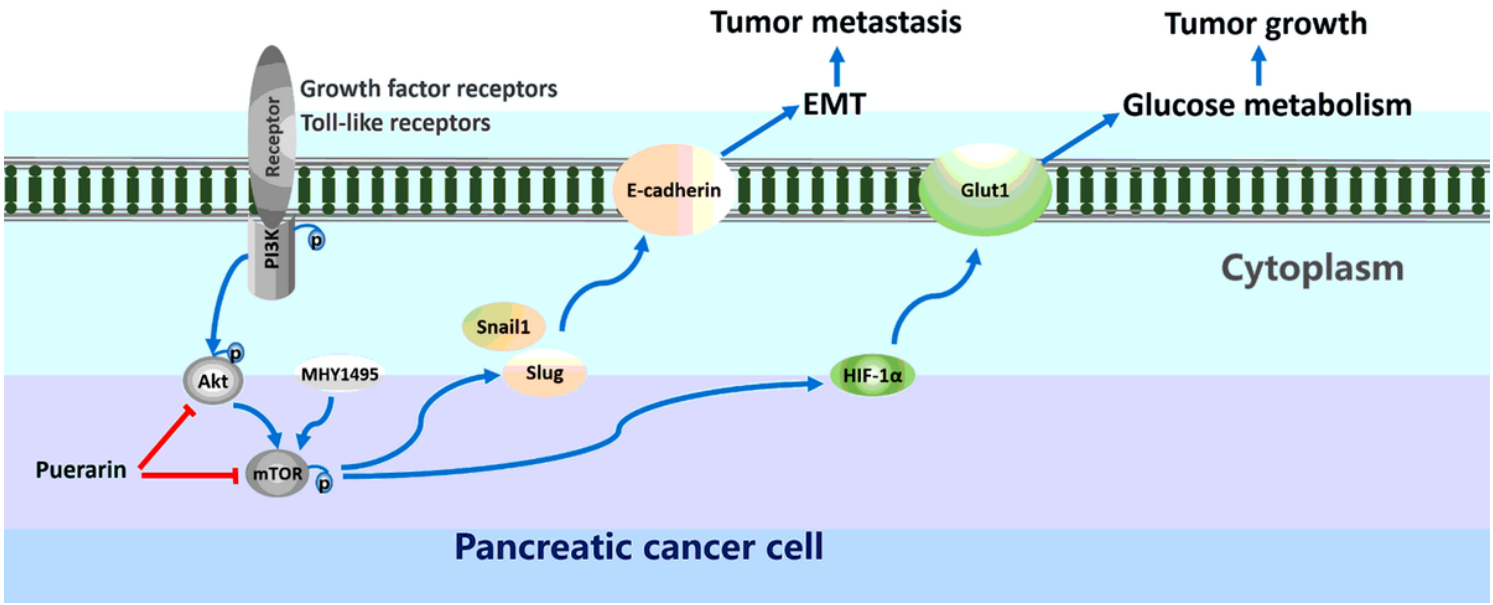

Figure 8

Puerarin suppresses oncogenesis and progression of PDAC via suppressing Akt/mTOR activity.